EPITHELIAL TRANSPORT

C. Madjdpour* · D. Bacic* · B. Kaissling · H. Murer ·
J. Biber

Segment-specific expression of sodium-phosphate cotransporters NaPi-IIa and -IIc and interacting proteins in mouse renal proximal tubules

Abstract Sodium-dependent phosphate cotransport in renal proximal tubules (PTs) is heterogeneous with respect to proximal tubular segmentation (S1 vs. S3) and nephron generation (superficial vs. juxtamedullary). In the present study, S1 and S3 segments of superficial and juxtamedullary nephrons were laser-microdissected and mRNA and protein expression of the Na/Pi-cotransporters NaPi-IIa and NaPi-IIc and the PDZ proteins NHERF-1 and PDZK1 determined. Expression of NaPi-IIa mRNA decreased axially in juxtamedullary nephrons. There was no effect of dietary Pi content on NaPi-lla mRNA expression in any proximal tubular segment. The abundance of the NaPi-IIa cotransporter in the brush-border membrane showed inter- and intranephron heterogeneity and increased in response to a low-Pi diet (5 days), suggesting that up-regulation of NaPi-lla occurs via post-transcriptional mechanisms. In contrast, NaPi-IIc mRNA and protein was up-regulated by the low-Pi diet in all nephron generations analysed. NHERF-1 and PDZK1, at both mRNA and protein levels, were distributed evenly along the PTs and did not change after a low-Pi diet.

Keywords Proximal tubule · Phosphate reabsorption · PDZ protein · Laser dissection · Immunostaining

*C. Madjdpour and D. Bacic contributed equally to this work

H. Murer · J. Biber (✉)
Institute of Physiology, University of Zürich,
Winterthurerstrasse 190,
8057 Zurich, Switzerland
e-mail: JuergBiber@access.unizh.ch
Tel.: +41-1-6355032
Fax: +41-1-6356814

C. Madjdpour* · D. Bacic* · B. Kaissling
Institute of Anatomy, University of Zurich,
8057 Zurich, Switzerland

Introduction

In kidneys, filtered inorganic phosphate (Pi) is reabsorbed mainly along the proximal tubules (PT). This process involves sodium-dependent phosphate (Na/Pi) cotransporters that are localized in the brush border membrane (BBM). The extent of Pi reabsorption in the PT is determined largely by the abundance of the Na/Pi-cotransporter NaPi-IIa (SLC34A1) [23]. Recently, a growth-related Na/Pi-cotransporter (NaPi-IIc; SLC34A3), which may play a role in renal phosphate absorption in weaning animals, has also been identified [25, 29]. Abundances of both NaPi-IIa and NaPi-IIc within the BBM are altered, for example, by parathyroid hormone and dietary intake of Pi [17, 18, 19, 27, 33, 34].

RT-PCR and in situ hybridization studies have shown NaPi-IIa mRNA expression only in the PT [3, 6, 27] and immunostaining for NaPi-IIa protein is also observed exclusively in the PT, albeit with an axial decrease of abundance (intranephron heterogeneity). Furthermore, the abundance of NaPi-IIa in BBM of PTs in juxtamedullary PTs is higher than in superficial nephrons (internephron heterogeneity) [6].

Recently, PDZ (postsynaptic protein P̲SD95, *Drosophila* protein d̲lg (discs large)-A and tight junction protein Z̲O-1) proteins that interact with NaPi-IIa have been identified [10]. Two of these, Na^+/H^+-exchanger regulatory factor-1 (NHERF-1) and PDZK1, are both localized in the brush border of the PT. They are assumed to play roles in the targeting and/or retrieval of NaPi-IIa to or from the apical membrane [1, 24]. Accordingly, the inter- and intranephron heterogeneity of NaPi-IIa may be related to segment- and nephron-specific differences of PT PDZK1 and NHERF-1 expression leading to quantitatively different trafficking processes and thus apical expression of NaPi-IIa. To address this question, we analysed the gene expression of NaPi-IIa and NaPi-IIc and of the PDZ proteins PDZK1 and NHERF-1 by the use of laser-assisted microdissection combined with quantitative real-time PCR and immunofluorescence staining in early (S1) and late (S3) PT segments of both superficial and juxtamedullary

nephrons. In addition, we examined the effect of different Pi dietary conditions on gene expression in the various PT segments.

Materials and methods

Slide preparation and laser-assisted microdissection

Eight-week-old male NMRI mice (Elevage Janvier, Le-Genest-Saint-Isle, France) were placed on a high- (1.2% Pi) or a low- (0.1% Pi) Pi diet for 5 days (three animals/group). The animals were then sacrificed and the kidneys removed immediately and snap frozen in liquid nitrogen. Cryosections (6 µm) were mounted on polyethylene membrane slides (Molecular Machines and Industries, Zürich, Switzerland). Tissue sections were allowed to thaw for 15 s, then immediately fixed for 30 s in 70% ethanol, 2×15 s in 95% ethanol and 2×15 s in 100% ethanol. Subsequently they were placed for 2×1 min in xylenes, mixed (ACS reagent, Sigma), air-dried for 4 min and finally placed on dry ice until microdissection.

Alternatively, for haematoxylin/eosin (HE) staining, sections were fixed in 70% ethanol for 30 s, then placed in Mayer's Haematoxylin solution (Sigma) for 30 s. After incubation in blueing solution (0.5% lithium carbonate) for 30 s, sections were rinsed in distilled water and placed in 70% ethanol for 30 s, then in alcoholic Eosin Y solution (Sigma) for 5 s. Afterwards sections were placed in 95% ethanol, 100% ethanol and Xylenes, mixed ACS reagent as described for unstained sections.

Laser microdissection was performed with an inverted microscope equipped with a motorised scanning stage and a solid-state laser in the UV region (Molecular Machines & Industries; see http://www.molecular-machines.com). The manufacturer's control software (UV CUT) allows the precise measurement of the dissected area in $µmetres^2$. Both S1 and S3 segments of superficial and juxtamedullary nephrons were identified by phase-contrast microscopy (Fig. 1) and a total area corresponding to $100,000 \pm 1,000$ $µm^2$ (approximately 30 segments each) was microdissected and collected for each sample. For the analysis of the expression of NaPi-IIc, strips of an area of 5,000,000 $µm^2$ of superficial cortex or deep cortex including outer stripe were microdissected.

RNA extraction and cDNA synthesis

RNA was extracted using the Absolutely RNA Nanoprep Kit (Stratagene) following the manufacturer's instructions. First-strand cDNA was synthesized using random hexamers and TaqMan Reverse Transcription Reagents (Applied Biosystems, Rotkreuz, Switzerland).

Quantitative real-time PCR

Relative quantitation of target gene mRNA was done using the ABI PRISM 7700 Sequence Detection System (Applied Biosystems). As an internal standard β-actin was chosen. The sequences of TaqMan probes (obtained from Biosearch Technologies, Novato, Calif., USA) and primers (obtained from Microsynth, Balgach, Switzerland) were as follows: 5′-(6-FAM) CCAGACACAACA-GAGGCTTCCACTTCTATGTC (BHQ-1)-3′ (probe), 5′-AGTCT-CATTCGGATTTGGTGTCA-3′ (forward), 5′-GCCGATGGCCTC-TACCCT-3′ (reverse) for NaPi-IIa, 5′-(6-FAM) CCAGCAAAA-GACCGAACTCTCAGCACAG (BHQ-1)-3′ (probe), 5′-TCTGCGGAGTCCGAGCAT-3′ (forward), 5′-TCAGAGTTAGAC-GAAGAGTGCGA-3′ (reverse) for PDZK1, 5′-(6-FAM) AC-CTGGATGGCCCCTTGCCTGA (BHQ-1)-3′ (probe), 5′-AGTG-CAAAGTGATCCCATCCC-3′ (forward), 5′-CCTTCTGTATC TCTCCATTGCTGAA-3′ (reverse) for NHERF-1, 5′-(6-FAM) CCACTTCTTCTTCAACCTGGCTGGCATACT (BHQ-1)-3′
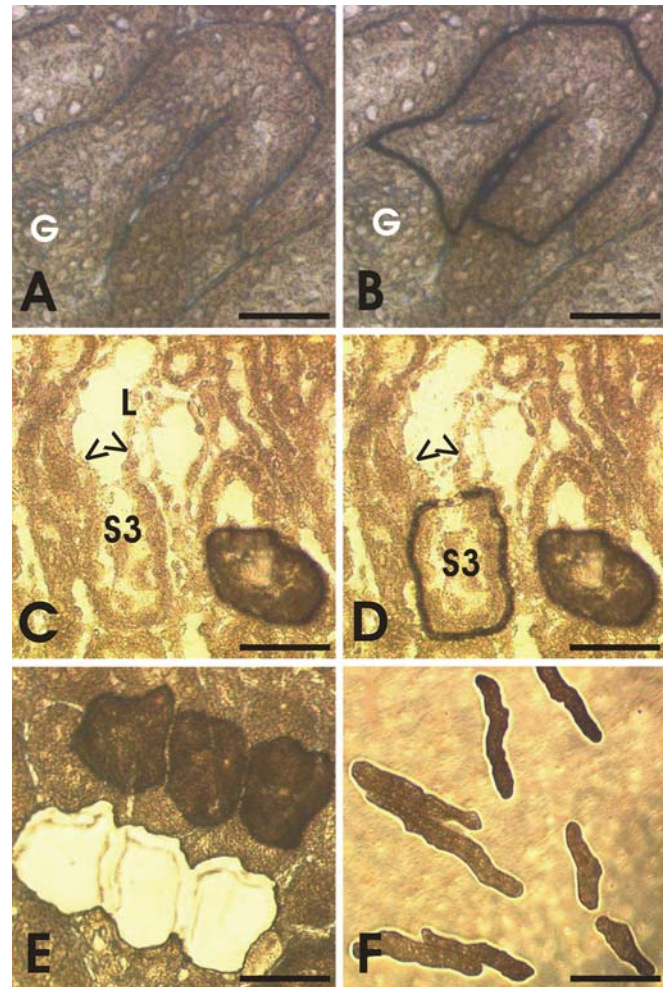

Fig. 1A–F Microdissection of proximal tubules. Upon removal, mouse kidneys were frozen immediately in liquid nitrogen. Cryosections (6 µm) were fixed in 70% ethanol and microdissected using phase-contrast microscopy to identify proximal tubular segments. **A** S1 segments were typically identified by their abrupt beginning at the urinary pole (*G* glomerulus). *Asterisks* indicate the course of the proximal tubule. **B**, **D** The laser left behind a thin black line in the tissue when cutting (*white arrowheads* in **B**). **C**, **D** Juxtamedullary S3 segments were selected in the outer stripe at the border to the inner stripe where transition to the descending thin limb (*DTL*) takes place (*black arrowheads*). The *white star* indicates a S3 segment that was already microdissected and transferred to the cap of the microdissection tube. **E** After cutting with the laser, the selected segments (*white asterisks*) were removed from their place of origin (*black asterisks*). **F** After completion of microdissection all the isolated tubules attached to the cap of the microdissection tube could be photographed on an empty area of the microdissection slide as shown by the example of superficial S3 segments. **A–E**: *Bar*=50 µm, **F** 100 µm

(probe), 5′-TAATCTTCGCAGTTCAGGTTGCT-3′ (forward), 5′-CAGTGGAATTGGCAGTCTCAAG-3′ (reverse) for NaPi-IIc and 5′-(6-FAM) CCATGAAGATCAAGATCATTGCTCCTCCT (BHQ-1)-3′ (probe), 5′-GACAGGATGCAGAAGGAGATTACTG-3′ (forward), 5′-CCACCGATCCACACAGAGTACTT-3′ (reverse) for β-actin.

For all genes primer concentrations were 900 nM and the probe concentration was 250 nM. TaqMan probes were located across exon-exon boundaries to exclude any amplification of genomic DNA. PCR reactions were performed using TaqMan Universal PCR Master Mix (Applied Biosystems) in a total reaction volume of

25 µl. Reaction conditions were: 2 min at 50 °C (uracil-*N*-glycosylase incubation), 10 min at 95 °C (activation of AmpliTaq Gold DNA polymerase) followed by 45 cycles of amplification (95 °C for 15 s and 60 °C for 1 min).

Relative expression was calculated according to user bulletin #2 of the ABI PRISM 7700 Sequence Detection System available at http://home.appliedbiosystems.com. Standard curves for target genes and β-actin were generated using total kidney mouse RNA.

Statistical methods

For PDZK1, NHERF-1 and NaPi-llc, mean expression values of the three animals per sample group were averaged and one-way ANOVA with Student-Newman-Keuls multiple comparisons test used for analysis. $P<0.05$ was taken as significant. Data are expressed as normalized expression means of three animals per group±SD.

Considerable variability of the expression of NaPi-lla mRNA between the different animals of the same group was observed. Therefore, data are presented for each animal separately as the mean of three determinations.

Immunofluorescence studies

Kidneys of mice that were treated identically as above were fixed and frozen as previously reported [8]. Cryosections (4 µm) were mounted on chrom alum/gelatine-coated glass slides and further processed for immunofluorescence.

For NaPi-IIa and NaPi-IIc immunofluorescence stainings, sections were pretreated for 10 min with 3% defatted milk powder and 0.02% Triton X-100 in PBS (blocking solution). After rinsing with PBS, sections were incubated with rabbit anti-rat polyclonal antiserum against the NaPi-IIa protein [6] or with an affinity purified anti-NaPi-llc antibody (kindly provided by Dr. K. Miyamoto; Japan). For immunofluorescence detection of PDZK1, sections were microwaved in buffer containing 0.01 M citrate in distilled water at 30% power for 10 min. After rinsing with PBS and covering for 10 min with blocking solution, sections were incubated with anti-PDZK1 antibody [10]. For NHERF-1 immunofluorescence staining, sections were pretreated with 1% SDS in PBS for 7 min. After repeated rinsing with PBS, they were covered for 10 min with blocking solution. Sections were then incubated with affinity-purified anti-NHERF-1 antibody (kindly provided by Dr. E. Weinman).

All primary antibodies were diluted in blocking solution and incubated overnight at 4 °C. Sections where then rinsed 3 times with PBS and incubated for 45 min at room temperature in the dark with the secondary antibody coupled to FITC or CY3. After rinsing with PBS, the sections were finally mounted using DAKO-Glycergel (Dakopatts, Glostrup, Denmark) containing 2.5% 1,4-diazabicyclo [2.2.2.]octane (DABCO; Sigma,) as a fading retardant, and studied on an epifluorescence microscope (Polyvar, Reichert-Jung, Austria).

Western blot analysis

PT brush borders of whole mouse cortex were isolated as described in [6] and the proteins (25 µg) were separated by SDS gel electrophoresis after denaturation by heating under reducing conditions (100 mM DTT, 2 min at 95 °C). After transfer onto nitrocellulose membranes, immunoblots were made [6] using the antibodies mentioned above. Immunoreactions were detected by enhanced chemiluminescence (ECL, SuperSignal, Pierce, Rockford, Ill., USA) and digital imaging (Diana lll, Raytest Straubenhardt, Germany). To ensure equal loading, transferred proteins were stained with Ponceau Rouge.

Results

Establishment of the method

HE staining has already been used in conjunction with laser-assisted microdissection of the kidney, however, this staining procedure may interfere with real-time PCR [2, 16, 22, 30]. We therefore first examined the effect of HE staining on the efficiency of real-time RT-PCR of all the target genes used in this study. To this end, 30 S1 segments of superficial nephrons corresponding to a total area of 100,000 µm² were microdissected and either stained or not. As illustrated in Fig. 2, amplification curves for NaPi-IIa of stained samples crossed the threshold 6–7 cycles later than the unstained samples; similar data were obtained for the amplification of NHERF-1 and PDZK1 (not shown). This suggested that prior staining impairs the efficiency of real-time RT-PCR, most likely due to lower recovery of total RNA. We therefore decided to micro-dissect unstained sections using phase-contrast microscopy as illustrated in Fig. 1.

NaPi-IIa expression

As illustrated in Fig. 3a, no axial heterogeneity of NaPi-lla mRNA expression was observed in superficial nephrons, whereas in juxtamedullary nephrons about 4–5 times less NaPi-IIa mRNA was present in S3 segments than in S1 segments. This expression profile was independent of the phosphate diet (1.2% or 0.1% Pi) given for 5 days, suggesting that altering the dietary Pi content does not influence transcription of NaPi-IIa mRNA. All expressions of NaPi-IIa mRNA are displayed relative to the content of β-actin mRNA, which was not significantly different between the different microdissected segments.
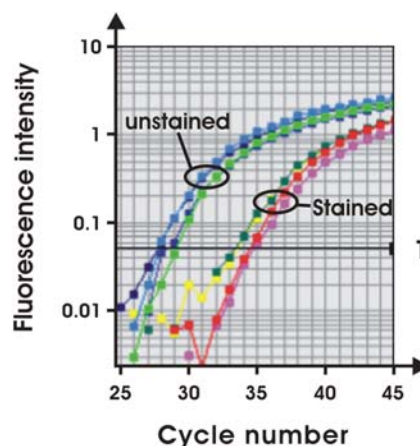

Fig. 2 Effect of haematoxylin/eosin (HE) staining on real-time RT-PCR efficiency. Thirty superficial S1 segments from either HE-stained or unstained kidney sections were microdissected, RNA isolated and real-time RT-PCR for NaPi-IIa performed. The amplification plot shown contains amplification curves in duplicates for two independent samples per group (*stained* amplification curves of samples from HE-stained tissue, *unstained* amplification curves of samples from unstained tissue, *T* threshold)

Fig. 3 Determination of segmental Na/P cotransporter-IIa (*NaPi-IIa*) mRNA (**a**) and protein (**b**) abundance. **a** NaPi-IIa mRNA from laser-microdissected S1 and S3 segments of superficial and juxtamedullary nephrons from mice fed a low- or high-Pi diet (*n*=3 mice/group) was isolated and quantified by real-time RT-PCR and expressed as the means of three determinations relative to β-actin for each animal. *Bars* representing values from the same animal are marked by *identical patterns*. (*juxt* juxtamedullary, *sup* superficial). **b** Kidneys of mice treated identically were perfusion-fixed and 4-μm cryosections immunostained for NaPi-IIa in S1 and S3 segments of both nephron generations. *Bar* ~10 μm
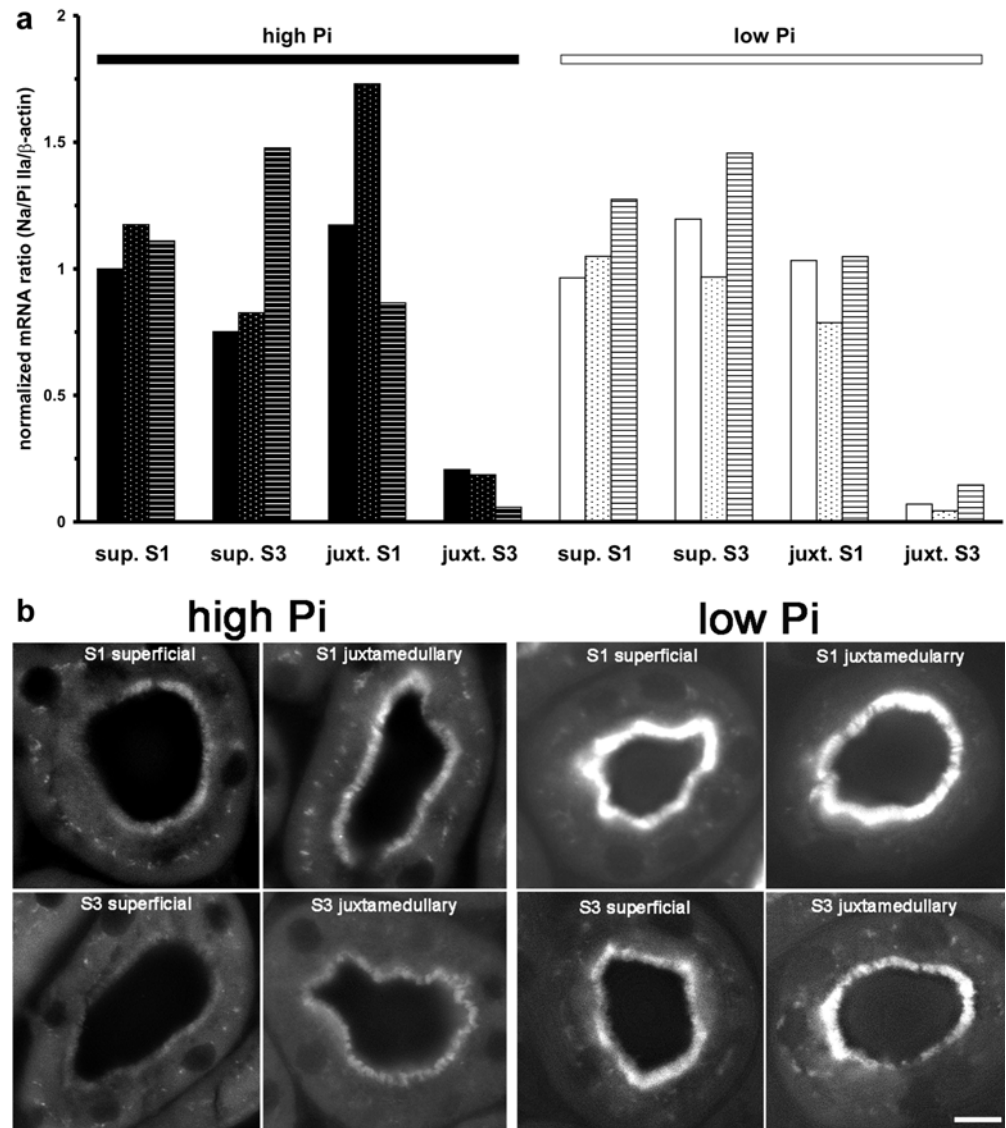
In contrast to the NaPi-IIa mRNA profiles, immunofluorescence staining for NaPi-IIa showed a clear decrease in intensity between the S1 and S3 segments of both nephron generations of high-Pi animals (Fig. 3b). Notably, NaPi-IIa was more abundant in the S3 segments of deep nephrons than in S3 segments of superficial nephrons, although the opposite was the case for the corresponding mRNA content. In addition, the low-Pi diet increased the abundance of NaPi-IIa in all segments. Consequently, inter- and intranephron heterogeneity of NaPi-IIa abundance was not as clear as in the high-Pi diet group.

Expression of NHERF-1 and PDZK1

Analysis of the expression of NHERF-1 and PDZK1 mRNA showed no significant differences between the different proximal tubular segments (Figs. 4a and 5a); nor were there any changes in the expressions of NHERF-1 or PDZK1 mRNA between the different Pi diets. Immuno-fluorescence staining showed equal intensities for NHERF-1 and PDZK1 in the brush borders of all examined segments of high- and low-Pi diet animals (Figs. 4b and 5b).

Expression of NaPi-IIc

We were not able to detect NaPi-IIc mRNA reliably in samples containing single microdissected tubules. To increase the amount of microdissected tissue, whole strips of tissue containing either superficial cortex or deep cortex together with outer stripe of the medulla were microdissected and analysed. In both Pi diet groups, significantly lower expression of NaPi-IIc mRNA (approximately 2-fold lower) was observed in strips containing juxtamedullary PTs than in strips containing superficial PTs (Fig. 6). The low-Pi diet caused a 137% increase ($P<0.001$) of NaPi-IIc mRNA in superficial cortical strips and a 72% increase in deep cortical strips ($P<0.05$).

Fig. 4 Na$^+$/H$^+$-exchanger regulatory factor-1 (*NHERF-1*) mRNA (**a**) and protein (**b**) expression and localization in the proximal tubule. **a** Kidneys of mice fed a high- or low-Pi diet were microdissected and S1 and S3 segments of superficial and juxtamedullary nephrons were isolated. RNA was extracted and quantified by real-time RT-PCR. *Bars* represent normalized expression; means±SD (*n*=3 mice). **b** Immunofluorescence studies for NHERF-1 protein in S1 and S3 segments of superficial and juxtamedullary nephrons. *Bar* ~10 μm
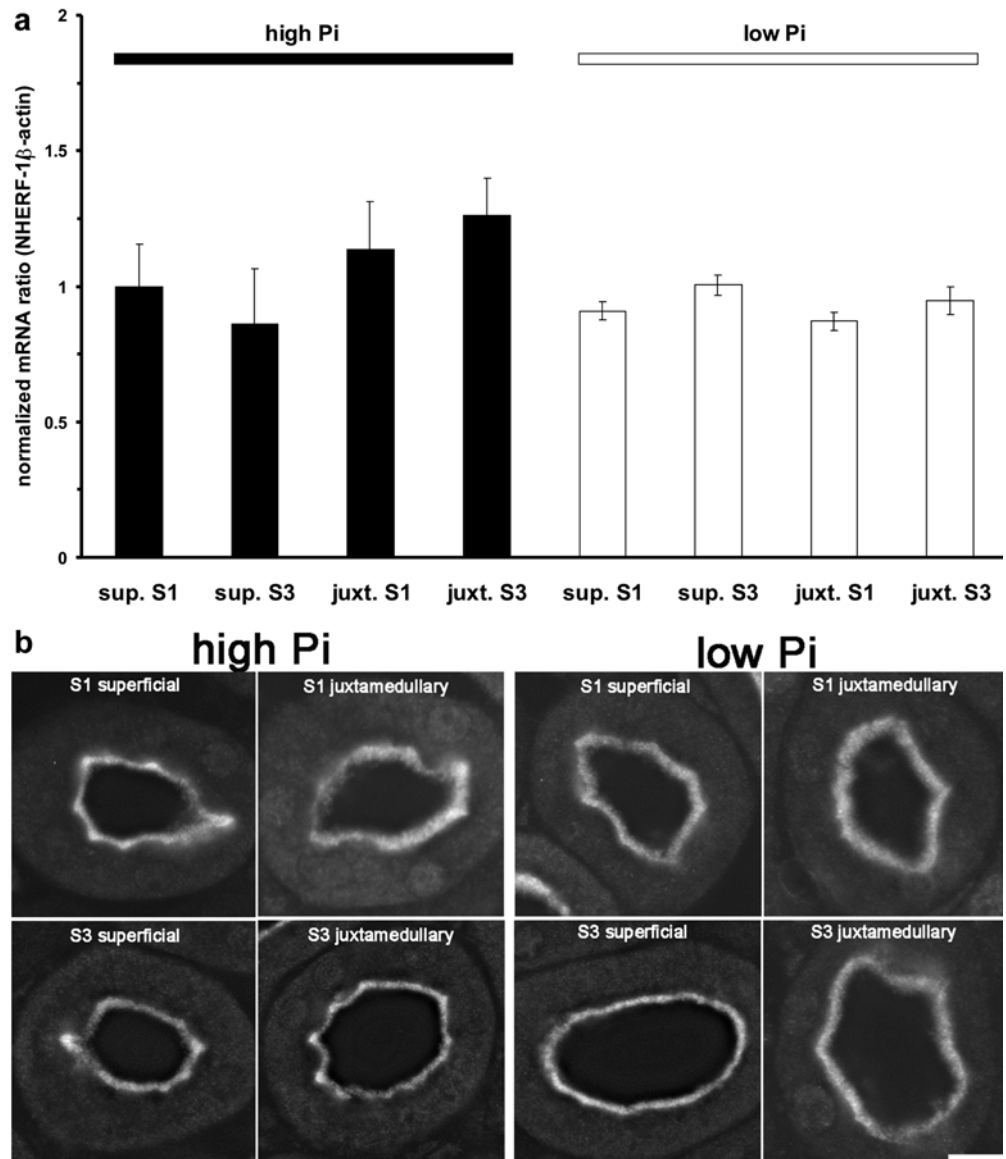
In high-Pi animals, immunofluorescence staining for NaPi-llc was detected in the juxtamedullary PTs only; no staining was observed in the superficial PTs (data not shown and [25]). As illustrated in Fig. 6b, in both superficial and juxtamedullary S1 segments, the low-Pi diet increased the expression of NaPi-llc, consistent with the results obtained by RT-PCR.

Western blots

To confirm the findings obtained by RT-PCR and immunofluorescence, BBMs were isolated from whole kidney cortex from animals fed a high- or low-Pi-diet and analysed by immunoblot (Fig. 7). In agreement with data shown above, the low-Pi diet increased the expression of NaPi-lla and NaPi-llc (approximately 2.5-fold and 5-fold respectively) but not that of NHERF 1 or PDZK1.

Discussion

Dependent on the relative abundance of a cell type of interest, analysis of gene expression in homogenates of heterogeneous tissues may result in an "averaging out" of expression. Recently, laser-capture microscopy has been introduced [9] and allows the recovery of single cells or cell populations for quantitative measurements of gene expression. Since then, a number of other laser-coupled microdissection devices have been developed and have proven to be of high precision and efficiency [4, 5, 35].

Reabsorption of phosphate exhibits considerable heterogeneity along different PTs and PT segments: Pi reabsorption in juxtamedullary nephrons is higher than in superficial nephrons [11, 12]. In agreement with its role in proximal tubular reabsorption of Pi [23], the abundance of the Na/Pi-cotransporter NaPi-IIa is highest in S1 segments of juxtamedullary nephrons and decreases axially along the PT [6]. In the present study, in animals

Fig. 5a, b Expression and localization of PDZK1. **a** Quantification of PDZK1 mRNA in S1 and S3 segments of superficial and juxtamedullary nephrons. *Bars* represent normalized expression; means ±SD (*n*=3 animals). **b** Immunofluorescence staining for PDZK1 protein. *Bar* ~10 μm
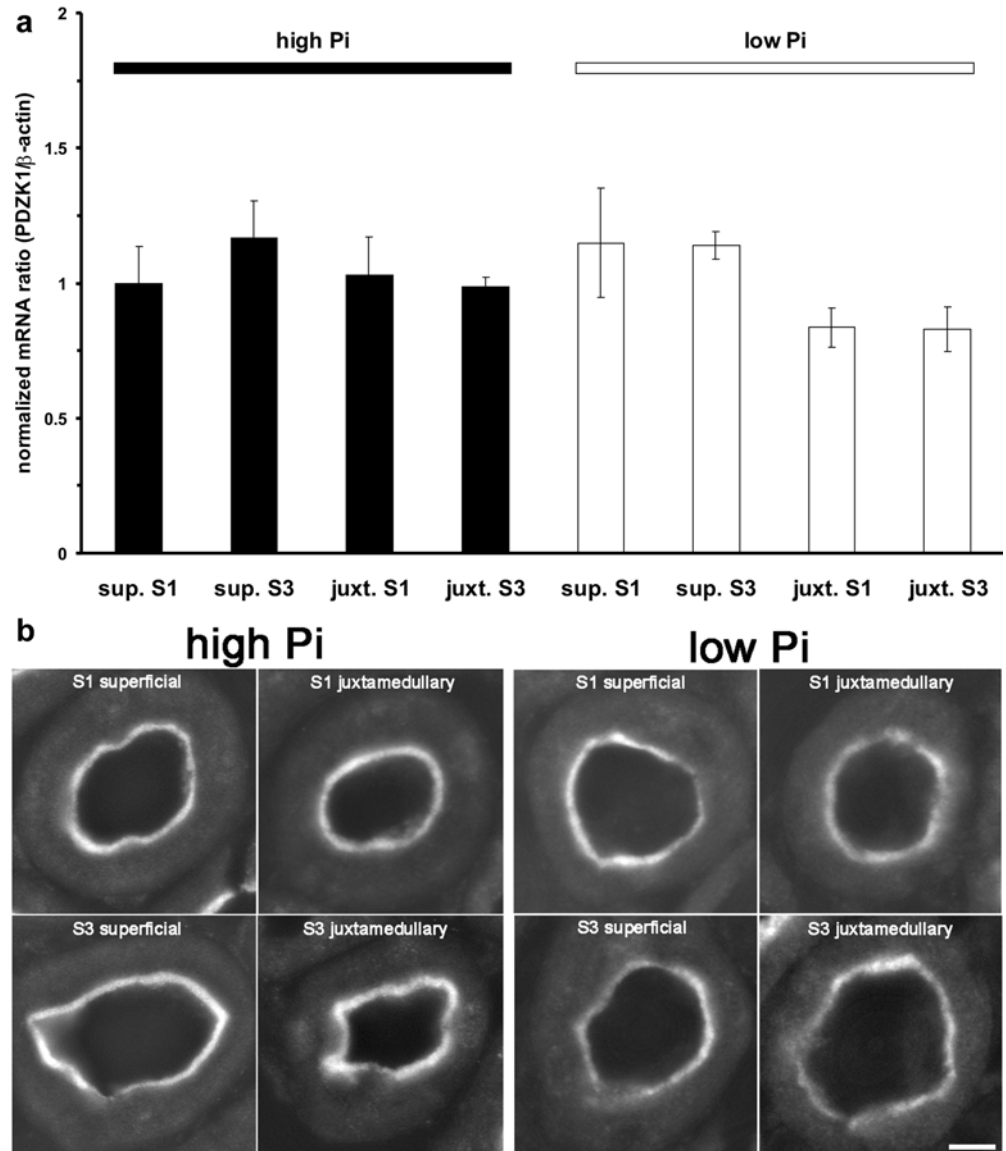
fed a high-Pi diet, the same pattern of heterogeneity of the abundance of the NaPi-IIa protein was observed. In contrast, NaPi-IIa mRNA was equally abundant in the S1 segments of superficial and juxtamedullary nephrons. Furthermore, an axial gradient of NaPi-IIa mRNA abundance from S1 to S3 segments was found only in juxtamedullary nephrons; in superficial PTs equal amounts of NaPi-IIa mRNA were detected in S1 and S3 segments. Thus, our studies clearly demonstrate that the abundances of NaPi-IIa protein and mRNA in mouse proximal tubules diverge.

Mechanisms involved in the regulation of NaPi-IIa-mediated renal reabsorption of Pi have been studied extensively. Most is known about the effects of dietary Pi content and the action of the parathyroid hormone (PTH) on the expression of NaPi-IIa [11, 17, 23]. In the present study we focussed on the chronic effect (5 days) of a low-compared with a high-Pi diet.

In agreement with earlier studies [17, 27], the content of NaPi-IIa protein increased in all PT segments of all

nephron generations. This was, however, not the case for the expression of NaPi-IIa mRNA. Although the abundance of NaPi-IIa mRNA in single nephrons varied considerably between different animals, the data shown in Fig. 3a demonstrate that the low-Pi diet did not alter NaPi-IIa mRNA expression, suggesting that in S1 and S3 PT segments of mice the apical abundance of NaPi-IIa is controlled post-transcriptionally rather than via an effect on transcription. The literature concerning the effect of a chronic changes in dietary Pi content on the expression of NaPi-IIa mRNA is not consistent. In rats, chronic deprivation of dietary Pi reportedly up-regulates NaPi-IIa mRNA [17, 27]. In contrast, studies in opossum kidney (OK) cells have shown that increased NaPi-IIa protein expression after alteration of the extracellular [Pi] can occur without the need for increased abundance of the mRNA [13, 26]. Moreover, in mice chronically fed a low-Pi diet, renal NaPi-IIa mRNA does not change [28, 32]. In contrast, other studies on mouse kidney tissue have shown

Fig. 6a, b Expression of NaPi-IIc in mouse kidney. **a** Quantification of NaPi-llc mRNA. Whole-kidney strips from mice fed either a high- or a low-Pi diet were microdissected and tissue strips obtained either from the superficial cortex or from the deep cortex including the outer stripe. *Bars* represent normalized expression; means±SD (n=3). *$P<0.05$, **$P<0.001$ vs. corresponding high-Pi diet (*OS* outer stripe). **b** Immunofluorescence staining for NaPi-llc protein in superficial and juxtamedullary mouse kidney cortex. *Bar* ~10 μm
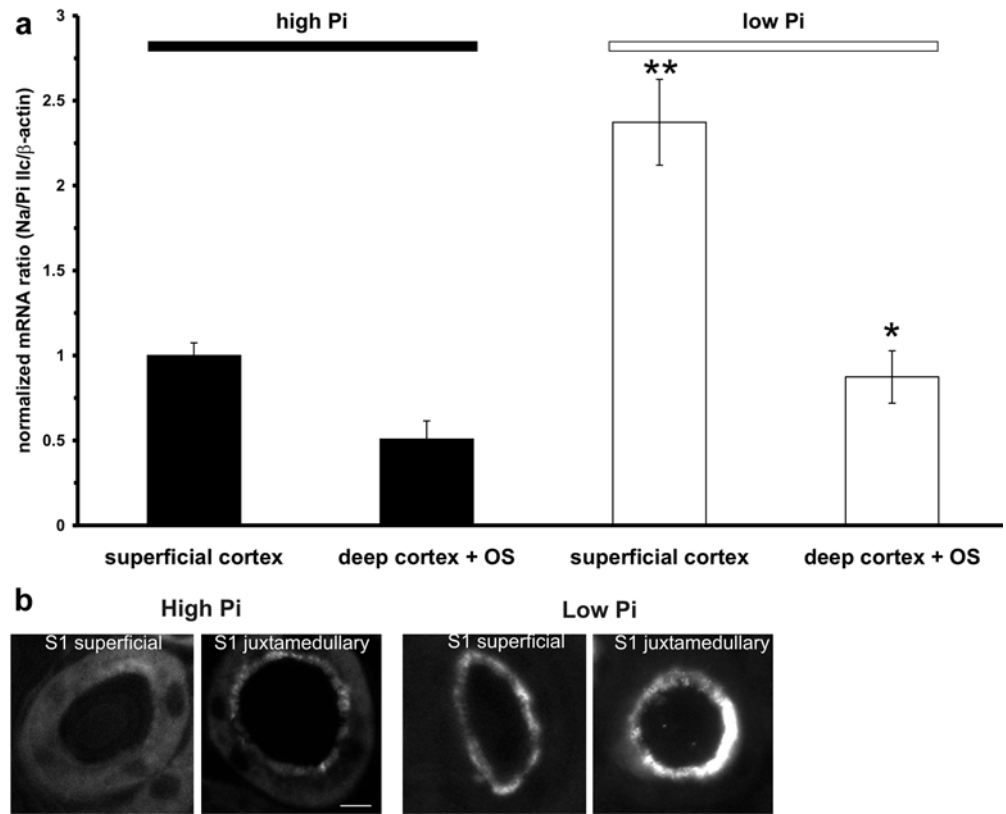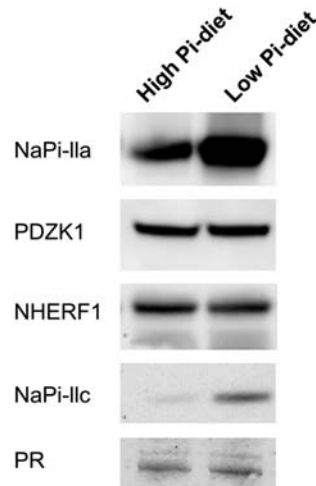

Fig. 7 Immunoblots of brush border membranes isolated from whole kidney cortex of mice fed a high- or a low-Pi diet. Blots were analysed for the abundance of the indicated proteins (*PR* Ponceau rouge staining of the β-actin band)

a low-Pi diet to increase NaPi-IIa mRNA to varying extents [14, 15, 19, 20, 21, 31].

Recently, a growth-related type II Na/Pi cotransporter (NaPi-IIc) has been identified in rat and mouse kidney. In weaning animals, NaPi-IIc immunostaining is present in PTs of superficial and juxtamedullary nephrons while in adult rat and mouse kidneys NaPi-IIc is found predominantly in the brush borders of juxtamedullary PTs [25, 29]. Our present study on the adult mouse kidney demonstrated that the mRNA of the Na/Pi-cotransporter NaPi-llc is present in both superficial and juxtamedullary nephrons and that NaPi-llc mRNA is increased by a low-Pi diet in both nephron generations (137% and 72% respectively). In

agreement, increased abundance of NaPi-llc was observed by Western blot analysis of brush border membranes isolated from the whole cortex. Thus, in contrast to the up-regulation of NaPi-lla, our data suggest that up-regulation of NaPi-llc in adult mice on a low-Pi diet occurs mainly by transcriptional mechanisms.

Besides the two Na/Pi-cotransporters NaPi-IIa and NaPi-IIc we assessed the mRNA and protein contents of two PDZ proteins (PDZK1 and NHERF-1), which are believed to interact with the NaPi-lla cotransporter [10]. These interactions, together with scaffolded regulatory elements such as PKA anchoring proteins, are thought to play important roles in the apical sorting, positioning and the regulation of NaPi-IIa [1]. On the basis of RT-PCR and immunohistochemistry, our results show that NHERF-1 and PDZK1 are expressed uniformly along the PTs of superficial and juxtamedullary nephrons. In addition, neither the mRNA nor the abundance (immunostaining intensity and Western blots) of these PDZ proteins were altered by a low-Pi diet. These data thus provide evidence that the expression of NHERF1 and PDZK1 is not regulated in parallel to that of NaPi-IIa. With respect to PDZK1 our findings contrast with two other reports. A recent study employing Western blot analysis has shown that the abundance of PDZK1 is up-regulated by a low-Pi diet [36]. At present we have no explanation for this discrepancy, although, different genetic backgrounds of the mice can be excluded since PDZK1 in C57Bl/6 mice also failed to respond a low-Pi diet (data not shown). In another study, diphor-1 (PDZK1, lacking one PDZ domain) was identified by a differential display of renal

cDNAs obtained from rats fed a high- or a low-Pi diet, indicating changes of diphor-1 mRNA [7]. It remains to be shown whether this apparent discrepancy between the present findings and the ones reported [7] is due to the different species used (mice or rats).

In summary, we have demonstrated the suitability of laser-assisted microdissection together with immunofluorescence microscopy for segment-specific analysis of gene expression in the PT. Gene expression profiles of NaPi-IIa, its interaction partners NHERF-1 and PDZK1 and of NaPi-IIc were generated with respect to their localization in renal PT and their possible regulation by a low-Pi diet. The data document a discrepancy between Na/Pi-cotransporter mRNA and protein contents, suggesting that post-transcriptional control mechanisms are of major importance in the adaptation to a low-Pi diet. In contrast, as NaPi-llc mRNA was up-regulated by low Pi-diet, regulation of NaPi-IIc may occur both transcriptionally and post-transcriptionally.

References

1. Biber J (2001) Emerging roles of transporter-PDZ complexes in renal proximal tubular reabsorption. Pflugers Arch 443:3–5
2. Burton MP, Schneider BG, Brown R, Escamilla-Ponce N, Gulley ML (1998) Comparison of histologic stains for use in PCR analysis of microdissected, paraffin-embedded tissues. Biotechniques 24:86–92
3. Collins JF, Gishan FK (1994) Molecular cloning, functional expression, tissue distribution and in situ hybridization of the renal sodium phosphate (Na/Pi) transporter in the control and hypophosphatemic mouse. FASEB J 8:862–868
4. Cornea A, Mungenast A (2002) Comparison of current equipment. Methods Enzymol 356:3–12
5. Curran SJ, McKay A, McLeod HL, Murray GI (2000) Laser capture microscopy. J Clin Pathol Mol Pathol 53:64–68
6. Custer M, Lötscher M, Biber J, Murer H, Kaissling B (1994) Expression of Na/Pi cotransport in rat kidney: localization by RT-PCR and immunhistochemistry. Am J Physiol 266:F767–F774
7. Custer M, Spindler B, Verrey F, Murer H, Biber J (1997) Identification of a new gene product (Diphor-1) regulated by dietary phosphate. Am J Physiol 273:F801–F806
8. Dawson TP, Gandhi R, Le Hir M, Kaissling B (1989) Ecto-5′-nucleotidase: localization in rat kidney by light microscopic histochemical and immunohistochemical methods. J Histochem Cytochem 37:39–47
9. Emmert-Buck MR, Bonner RF, Smith PD, Chuaqui RF, Zhuang Z, Goldstein SR, Weiss RA, Liotta LA (1996) Laser capture microdissection. Science 274:998–1001
10. Gisler SM, Stagljar I, Traebert M, Bacic D, Biber J, Murer H (2001) Interaction of the type II Na/Pi cotransporter with PDZ proteins. J Biol Chem 276:9206–9213
11. Haas JA, Berndt T, Knox FG (1978) Nephron heterogeneity of phosphate reabsorption. Am J Physiol 234:F287–F290
12. Haramati A (1985) Tubular capacity for phosphate reabsorption in superficial and deep nephrons. Am J Physiol 248:F729–F733
13. Hilfiker H, Hartmann CM, Stange G, Murer H (1998) Characterization of the 5′-flanking region of OK cell type II Na-Pi cotransporter gene. Am J Physiol 274:F197–F204
14. Hoag MH, Martel J, Gauthier C, Tenenhouse HS (1999) Effects of Npt2 gene ablation and low-phosphate diet on renal Na+/phosphate cotransport and cotransporter gene expression. J Clin Invest 104:679–686
15. Kido S, Miyamoto K, Mizobuchi H, Taketani Y, Ohkido I, Ogawa N, Kaneko Y, Harashima S, Takeda E (1999). Identification of regulatory sequences and binding proteins in the type II sodium/phosphate cotransporter NPT2 gene responsive to dietary phosphate. J Biol Chem 274:28256–28263
16. Kohda Y, Murakami H, Moe OW, Star RA (2000) Analysis of segmental renal gene expression by laser capture microdissection. Kidney Int 57:321–331
17. Levi M, Lötscher M, Sorribas V, Custer M, Arar M, Kaissling B, Murer, Biber J (1994) Cellular mechanisms of acute and chronic adaptation of rat renal Pi transporter to alterations in dietary Pi. Am J Physiol 267:F900–F908
18. Lötscher M, Kaissling B, Biber J, Murer H, Levi M (1997) Role of microtubules in the rapid regulation of renal phosphate transport in response to acute alterations in dietary phosphate content. J Clin Invest 99:1302–1312
19. Lötscher M, Scarpetta Y, Levi M, Halaihel N, Wang H, Zajicek HK, Biber J, Murer H, Kaissling B (1999) Rapid down-regulation of rat renal Na/Pi cotransporter in response to parathyroid hormone involves microtubule rearrangement. J Clin Invest 104:483–494
20. Miyamoto K, Itho M (2001) Transcriptional regulation of the NPT2 gene by dietary phosphate. Kidney Int 60:412–415
21. Morita K, Fujioka A, Haga H, Nii T, Segawa H, Kouda T, Taketani Y, Hisano S, Fukui Y, Miyamoto K, Takeda E (1998) Dietary regulation of renal phosphate transporters in hypophosphatemic mice. J Bone Miner Metab 16:234–240
22. Murase T, Inagaki H, Eimoto T (2000) Influence of histochemical and immunohistochemical stains on polymerase chain reaction. Mol Pathol 13:147–151
23. Murer H, Hernando N, Forster I, Biber J (2000) Proximal tubular phosphate reabsorption: molecular mechanisms. Physiol Rev 80:1373–1409
24. Murer H, Hernando N, Forster I, Biber J (2003) Regulation of Na/Pi transporter in the proximal tubule. Annu Rev Physiol 65:531–542
25. Ohkido I, Segawa H, Yanagida R, Nakamura M, Miyamoto K (2003) Cloning, gene structure and dietary regulation of the type-llc Na/Pi cotransporter in the mouse kidney. Pflugers Arch 446:186–115
26. Pfister MF, Hilfiker H, Forgo J, Lederer E, Biber J, Murer H (1998) Cellular mechanisms involved in the acute adaptation of OK cell Na/Pi-cotransport to high- or low-Pi medium. Pflugers Arch 435:713–719
27. Ritthaler T, Traebert M, Lötscher M, Biber J, Murer H, Kaissling B (1999) Effects of phosphate intake on distribution of type II Na/Pi cotransporter mRNA in rat kidney. Kidney Int 55:976–983
28. Roy S, Martel J, Tenenhouse HS (1997) Growth hormone normalizes renal 1,25-dihydroxyvitamin D3-24-hydroxylase gene expression but not Na+-phosphate cotransporter (Np2) mRNA in phosphate-deprived Hyp mice. J Bone Miner Res 12:1672–1680
29. Segawa H, Kaneko I, Takahashi A, Kuwahata M, Ito M, Ohkido I, Tatsumi S, Miyamoto K (2002) Growth-related renal type II Na-Pi cotransporter. J Biol Chem 277:19665–19672
30. Serth J, Kuczyk MA, Paeslack U, Lichtinghagen R, Jonas U (2000) Quantification of DNA extracted after micropreparation of cells from frozen and formalin-fixed tissue sections. Am J Pathol 156:1189–1196
31. Tenenhouse HS, Martel J, Biber J, Murer H (1995) Effect of Pi restriction on renal Na+-Pi cotransporter mRNA and immunoreactive protein in X-linked Hyp mice. Am J Physiol 268:F1062–F1069

32. Tenenhouse HS, Roy S, Martel J, Gauthier C (1998) Differential expression, abundance, and regulation of Na^+-phosphate cotransporter genes in murine kidney. Am J Physiol 275:F527–F534

33. Traebert M, Völkl H, Biber J, Murer H, Kaissling B (2000) Luminal and contraluminal action of 1–34 and 3–34 PTH peptides on renal type II $Na-P_i$ cotransporter. Am J Physiol 278:F792–F798

34. Traebert M, Roth J, Biber J, Murer H, Kaissling B (2000) Internalization of proximal tubular type II $Na-P_i$ cotransporter by PTH: immunogold electron microscopy. Am J Physiol 278:F148–F154

35. Walch A, Specht K, Smida J, Aubele M, Zitzelsberger H, Höfler H, Werner M (2001) Tissue microdissection techniques in quantitative genome and gene expression analyses. Histochem Cell Biol 115:269–276

36. Weinman EJ, Boddeti A, Cunningham R, Akom M, Wang F, Wang Y, Liu J, Steplock D, Shenolikar S, Wade JB (2003) NHERF-1 is required for renal adaptation to a low-phosphate diet. Am J Physiol 285:F1225–F1232